Crystal Structures and Thermal Behavior of Bis(dibenzyldimethylammonium) Tetrabromometallates(II) [*M* = Mn(II), Co(II) and Zn(II)] and Their Solvates

Sara Busi[a], Roland Fröhlich[b], Manu Lahtinen[a], Reijo Sillanpää[a], and Kari Rissanen[a]

[a] Department of Chemistry, University of Jyväskylä, P.O.Box 35, FIN–40014 University of Jyväskylä, Finland
[b] Organisch-Chemisches Institut, Universität Münster, Corrensstrasse 40, 48149 Münster, Germany

Reprint requests to S. Busi. Fax: +358 14 2602501. E-mail: gibusi@cc.jyu.fi

Z. Naturforsch. **2007**, *62b*, 35 – 43; received August 14, 2006

Six new A_2MBr_4 structures [A = dibenzyldimethylammonium cation, M = Mn(II), Co(II) or Zn(II)] were crystallized with or without solvent molecules from acetonitrile, methanol and/or aqueous solutions. The isomorphous compounds $[(Bz_2Me_2N)_2][MnBr_4]\cdot CH_3CN\cdot H_2O$ (**1**) and $[(Bz_2Me_2N)_2][ZnBr_4]\cdot CH_3CN\cdot H_2O$ (**4**) crystallize in the triclinic space group $P1$ from acetonitrile solutions. The solvent molecules participate in the hydrogen bonding network inside the crystal structure. $[(Bz_2Me_2N)_2][CoBr_4]\cdot 0.5CH_3CN$ (**2**) crystallizes from an acetonitrile solution in the monoclinic space group $P2_1/c$. The solvent molecules fill the voids of the crystal structure. Compound **2** is isostructural with the previously reported compounds $[(Bz_2Me_2N)_2][MCl_4]\cdot 0.5CH_3CN$ with M = Mn(II), Co(II), Ni(II), Cu(II) or Zn(II). $[(Bz_2Me_2N)_2][CoBr_4]$ (**3**) and $[(Bz_2Me_2N)_2][ZnBr_4]$ (**5a**) crystallize from a methanol solution in the monoclinic space group $P2_1/c$ without solvents. A polymorph of compound **5a**, $[(Bz_2Me_2N)_2][ZnBr_4]$ (**5b**), was crystallized from aqueous solution in the monoclinic space group $P2_1/c$. The packing of the components of the two polymorphs differs clearly. One cation of **5a** appears in the W-conformation whereas the other cation of **5a** and both cations of **5b** appear in twisted conformations. In addition to the ionic interactions between the ion pairs, the packing of the compounds is stabilized by hydrogen bonds and weak intermolecular π–π interactions in all cases. The compounds melt around 200 °C and decompose mainly in two steps just above the melting point. Slow evaporation of solvents is observed both in the TG and DSC diagrams of the solvates (**1**, **2** and **4**) below 100 °C.

Key words: Quaternary Ammonium Compound, Tetrabromometallate, Tetrahalometallate, X-Ray Single Crystal Diffraction, Thermal Analysis

Introduction

The general interest in $[A]_2[MX_4]$ structures with A = organic cation, M = transition metal ion and X = halide (Cl, Br or I) lies in their wide structural variability [1 – 5], several phase transitions [2, 6 – 9], modulated phases [10 – 15], thermochromic behavior [16 – 18] and magnetic properties in the solid state [19 – 24]. The renewed notice has focused on complex magnetic systems, such as spin ladders and alternating exchange chains [23, 25, 26].

By varying the cations or the transition metal and the halogen (X = Cl, Br, or I) in the $MX_4{}^{2-}$ anion, different kinds of packing motifs are obtained. The first-row transition metals have an ability to form a large range of complexes with mainly tetrahedral and square planar stereochemistry [27 – 32]. For M = Mn(II), Fe(II), Co(II), Ni(II), Zn(II) the tetrahedral geometry is common [3, 33 – 39]. Instead, when M is copper(II), additional flexibility is brought into the system, because the Cu ion undergoes a Jahn-Teller distortion of its tetrahedral coordination geometry [27]. Thus, the tetrahedral $CuX_4{}^{2-}$ ion flattens toward D_{2d} symmetry. The geometry of the $MX_4{}^{2-}$ anions in the solid state is influenced by many other factors, such as the electrostatic repulsion between the halide ions, the packing forces as well as hydrogen bonding between the cations and anions [40]. The hydrogen bonding removes charge from the halogen atoms and thus reduces the electrostatic repulsions between these atoms, which allows the movement of anions toward the square planar geometry [16, 41, 42].

The tetrabromocuprate(II) anion is expected to have a larger dihedral angle (the measure of the distor-

Table 1. Crystallographic data for compounds **1** – **5** at 173(2) K.

Compound	**1**	**2**	**3**	**4**	**5a**	**5b**
Formula	$(C_{16}H_{20}N)_2MnBr_4$ $\cdot CH_3CN\cdot H_2O$	$(C_{16}H_{20}N)_2CoBr_4$ $\cdot 0.5CH_3CN$	$(C_{16}H_{20}N)_2CoBr_4$	$(C_{16}H_{20}N)_2ZnBr_4$ $\cdot CH_3CN\cdot H_2O$	$(C_{16}H_{20}N)_2ZnBr_4$	$(C_{16}H_{20}N)_2ZnBr_4$
M_r [g mol^{-1}]	886.31	851.76	831.23	896.74	837.67	837.67
Crystal system	triclinic	monoclinic	monoclinic	triclinic	monoclinic	monoclinic
Space group	$P\bar{1}$	$P2_1/c$	$P2_1/c$	$P\bar{1}$	$P2_1/c$	$P2_1/c$
a [Å]	9.169(2)	14.368(3)	17.057(3)	9.121(2)	17.049(3)	13.768(3)
b [Å]	13.201(3)	16.401(3)	9.171(2)	13.218(3)	9.171(2)	12.974(3)
c [Å]	15.639(3)	15.966(3)	23.227(5)	15.591(3)	23.219(5)	19.510(4)
α [°]	83.93(3)	90	90	83.74(3)	90	90
β [°]	88.39(3)	108.70(3)	109.75(3)	88.03(3)	109.70(3)	103.28(3)
γ [°]	77.68(3)	90	90	77.46(3)	90	90
V [Å^3]	1838.8(6)	3564(2)	3420(2)	1824(1)	3418(2)	3392(2)
Z	2	4	4	2	4	4
ρ_{calcd} [g cm^{-3}]	1.60	1.59	1.62	1.63	1.63	1.64
μ [mm^{-1}]	4.74	4.99	5.20	5.09	5.42	5.46
$F(000)$	886	1696	1652	896	1664	1664
Crystal size [mm]	0.30×0.20×0.10	0.10×0.10×0.10	0.25×0.20×0.20	0.20×0.10×0.04	0.40×0.20×0.20	0.15×0.10×0.02
θ range [°]	2.48 – 28.14	2.83 – 28.12	1.27 –25.36	2.63 – 25.24	1.27 – 28.10	2.58 – 25.34
Reflections collected	14411	15168	10047	11706	13780	11956
Independent reflections	8862	8299	6200	6536	8151	6210
Data/Restraints/Params	8862 / 3 / 400	8299 / 0 / 380	6200 / 0 / 357	6536 / 3 / 399	8151 / 0 / 357	6210 / 0 / 356
GooF	1.072	1.090	1.224	1.051	1.078	1.057
R(int)	0.0466	0.0661	0.0515	0.0644	0.0544	0.0639
Final R indices, $R1/wR2$ $[I \geq 2\sigma(I)]$	0.0585 / 0.1006	0.0582 / 0.0861	0.0641 / 0.1455	0.0541 / 0.0961	0.0447 / 0.0761	0.0443 / 0.0758
R indices, $R1/wR2$ (all data)	0.1005 / 0.1183	0.1167 / 0.1032	0.0963 / 0.1717	0.0915 / 0.1106	0.0767 / 0.0880	0.0731 / 0.0846
Largest diff.peak / hole [e Å^{-3}]	0.933 / −0.989	0.496 / −0.498	1.034 / −0.909	0.866 / −0.751	0.967 / −0.895	0.479 / −0.525

tion from square planar) than the tetrachlorocuprate(II) anion because of the distortion towards a tetrahedral geometry will lessen ligand-ligand repulsions for the larger Br atoms [42, 43].

Our interest has been to examine the effect of the metal atom on the packing of $[A]_2[MX_4]$ complexes by using the same cation (A = dibenzyldimethylammonium cation) and varying the first-row transition metal cation (M = Mn, Fe, Co, Ni, Cu or Zn) and the halide ion (X = Br or Cl). In this paper, we present the crystal structures and thermal behavior of six $[(Bz_2Me_2N)_2][MBr_4]$ (M = Mn, Co or Zn) complexes and compare these properties with those previously reported for $[(Bz_2Me_2N)_2][MCl_4]$ (M = Mn, Co, Ni, Cu or Zn) analogs [44, 45].

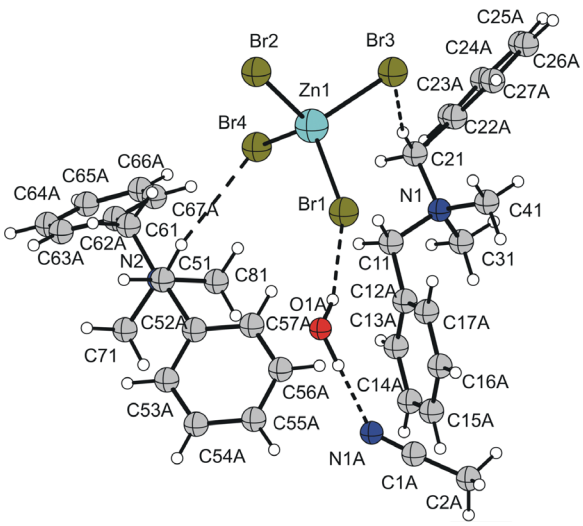

Fig. 1. The crystal structure and labelling scheme of compound **4** as an example of the isomorphous compounds **1** and **4** containing one acetonitrile and one water molecule in the asymmetric unit.

Results and Discussion

X-Ray structure analyses

Crystallographic data and selected bond lengths and angles of the new structures are presented in Tables 1 and 2. Compounds **1**, **2** and **4** crystallize as solvates,

Table 2. Selected bond lengths (Å) and angles (°) of compounds **1** – **5**, M = Mn (**1**), Co (**2** – **3**) or Zn (**4** – **5**).

Compound	**1**	**2**	**3**	**4**	**5a**	**5b**
N(1)–C(11)	1.540(6)	1.523(6)	1.543(10)	1.529(7)	1.531(5)	1.536(6)
N(1)–C(21)	1.542(6)	1.540(7)	1.521(10)	1.520(8)	1.525(5)	1.516(6)
N(1)–C(31)	1.494(6)	1.496(7)	1.486(10)	1.499(7)	1.498(5)	1.502(6)
N(1)–C(41)	1.490(6)	1.496(7)	1.491(10)	1.504(7)	1.496(5)	1.510(6)
N(2)–C(51)	1.541(6)	1.534(6)	1.534(10)	1.534(7)	1.526(5)	1.523(6)
N(2)–C(61)	1.535(6)	1.529(7)	1.515(9)	1.522(8)	1.527(5)	1.531(6)
N(2)–C(71)	1.501(6)	1.485(6)	1.498(9)	1.507(8)	1.495(5)	1.504(6)
N(2)–C(81)	1.498(6)	1.501(7)	1.495(10)	1.494(8)	1.493(5)	1.503(6)
M–Br(1)	2.499(2)	2.418(1)	2.414(2)	2.411(2)	2.428(1)	2.418(1)
M–Br(2)	2.502(2)	2.387(1)	2.423(2)	2.420(2)	2.413(2)	2.434(1)
M–Br(3)	2.502(2)	2.409(2)	2.412(2)	2.408(2)	2.396(1)	2.403(1)
M–Br(4)	2.509(2)	2.434(1)	2.399(2)	2.411(2)	2.415(1)	2.410(1)
Average of M–X	2.503	2.412	2.412	2.413	2.413	2.416
C(11)–N(1)–C(21)	106.6(3)	106.0(4)	105.7(6)	105.8(5)	109.9(3)	109.8(4)
C(11)–N(1)–C(31)	110.3(4)	110.9(4)	109.7(6)	110.7(5)	106.7(3)	110.9(4)
C(11)–N(1)–C(41)	110.0(4)	110.1(4)	110.2(6)	109.8(5)	109.7(3)	106.0(4)
C(21)–N(1)–C(31)	110.2(4)	109.2(4)	111.1(6)	109.7(5)	110.8(3)	111.0(4)
C(21)–N(1)–C(41)	110.3(4)	110.9(4)	110.6(7)	111.5(5)	110.9(3)	110.4(4)
C(31)–N(1)–C(41)	109.5(4)	109.8(4)	109.5(7)	109.2(5)	108.7(3)	108.6(4)
C(51)–N(2)–C(61)	105.5(3)	104.9(4)	109.9(6)	106.1(4)	105.7(3)	109.6(4)
C(51)–N(2)–C(71)	110.0(4)	111.3(4)	109.3(6)	109.8(5)	110.9(3)	110.9(4)
C(51)–N(2)–C(81)	109.6(4)	110.1(4)	106.6(6)	110.8(5)	109.9(3)	110.5(4)
C(61)–N(2)–C(71)	110.9(4)	109.6(5)	112.0(6)	110.0(5)	110.4(3)	106.5(4)
C(61)–N(2)–C(81)	110.6(4)	112.1(5)	110.0(6)	110.8(5)	110.5(3)	110.6(4)
C(71)–N(2)–C(81)	110.2(4)	108.8(4)	108.7(6)	109.3(5)	109.3(3)	108.7(4)
Br(1)–M–Br(2)	107.72(5)	108.20(4)	110.46(6)	109.61(5)	110.12(3)	102.76(3)
Br(1)–M–Br(3)	108.44(5)	109.03(4)	109.60(6)	108.15(5)	110.13(3)	113.16(3)
Br(1)–M–Br(4)	109.23(5)	109.70(4)	108.28(5)	110.40(5)	107.09(3)	108.56(3)
Br(2)–M–Br(3)	110.51(5)	114.92(4)	107.23(5)	109.70(5)	108.82(3)	107.00(3)
Br(2)–M–Br(4)	111.25(4)	108.95(4)	110.19(6)	110.54(4)	109.56(3)	113.80(4)
Br(3)–M–Br(4)	109.62(5)	105.96(4)	111.08(5)	108.39(5)	111.11(3)	111.36(4)
Average of two largest Br–M–Br	110.88	112.31	110.77	110.47	110.62	113.48
Solvents:						
N(1A)–C(1A)–C(2A)	178(2)	175(3)		177(2)		
H(1AA)–O(1A)–H(1AB)	108(2)					

whereas compounds **3**, **5a** and **5b** crystallize without solvents.

Compounds **1** and **4** are isomorphous and they crystallize in the triclinic space group $P\bar{1}$. The molecular structure of **1** is presented in Fig. 1. The asymmetric unit consists of one $MnBr_4{}^{2-}$ dianion, two $Bz_2Me_2N^+$ cations, one acetonitrile and one water molecule. Both cations are in the W-conformation.

The crystal structures of **1** and **4** are stabilized by C–H···Br$^-$ (C–H···Br$^-$ < 3.0 Å), O–H···N and O–H···Br$^-$ hydrogen bonds. The hydrogen bonding and the packing of **1** and **4** are presented in Fig. 2. Each anion forms five C–H···Br$^-$ bonds with four nearest cations and one acetonitrile molecule. The anion forms one O–H···Br$^-$ bond with a water molecule, which is further bonded to an acetonitrile molecule by an O–H···N hydrogen bond. Thus the solvent molecules are participating in the hydrogen bonding network, and are not just filling the voids inside the crystal structure.

Between the cations, weak π–π interactions, both face to face and edge to face interactions, help to stabilize the packing of the components. The geometry of the $MX_4{}^{2-}$ anions is close to tetrahedral.

Compound **2** crystallizes in the monoclinic space group $P2_1/n$ with $Z = 4$. The molecular structure is presented in Fig. 3. The asymmetric unit consists of one dianion, two $Bz_2Me_2N^+$ cations and one half of an acetonitrile molecule. Both cations are in the W-conformation. The acetonitrile molecule fills the voids of the crystal structure. Hydrogen bonds (especially weak C–H···Br$^-$ hydrogen bonds) between the acetonitrile molecule and the tetrahalometallate salt are not discernible.

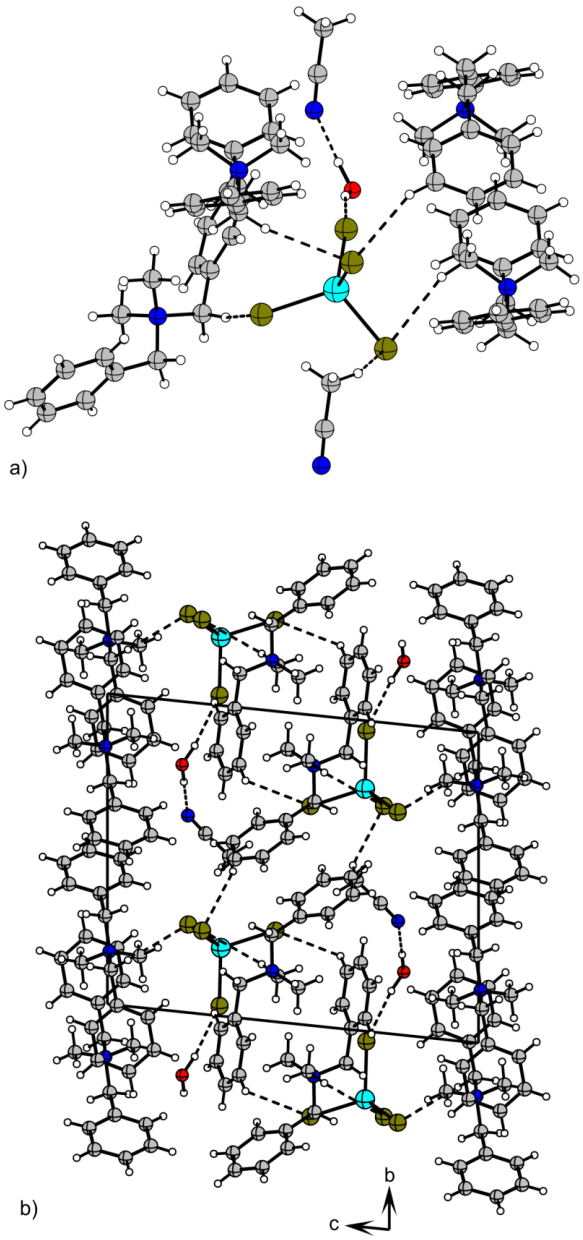

Fig. 2. a) The hydrogen bonding around the $ZnBr_4^{2-}$ anion of **4**. The C–H···Br$^-$ bond lengths are 2.86(1) – 2.98(4) Å, shown as dashed lines. O–H···N and O–H··· Br$^-$ bond lengths are 1.82(11) and 2.34(8) Å, respectively. b) The packing of isostructural compounds **1** (M = Mn) and **4** (M = Zn) viewed along the crystallographic a axis. The hydrogen bonds (C–H···Br$^-$ < 3.0 Å) are shown as dashed lines.

The packing of **2** is presented in Fig. 4. The ion pairs form C–H···Br$^-$ hydrogen bonds and weak edge to face π–π interactions of the phenyl groups. Each anion

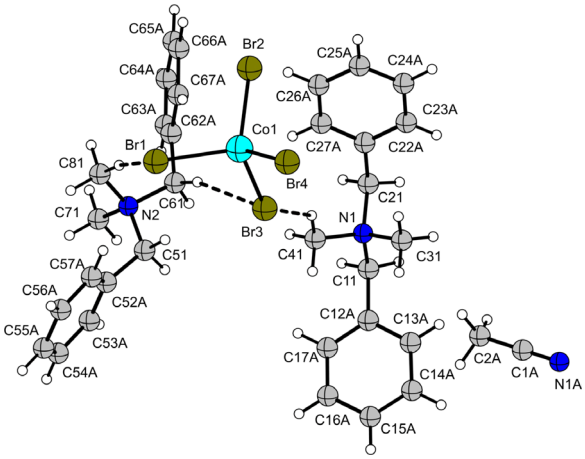

Fig. 3. The crystal structure of compound **2**. The hydrogen bonds (Br$^-$···H–C < 3.0 Å) are shown as dashed lines.

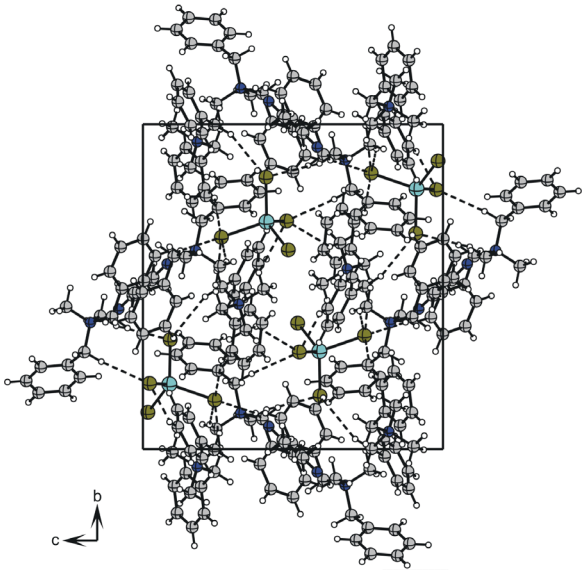

Fig. 4. The packing of compound **2** viewed along the crystallographic a axis. The hydrogen bonds (C–H···Br$^-$ < 3.0 Å) are shown as dashed lines.

forms ten C–H···Br$^-$ hydrogen bonds (C–H···Br$^-$ < 3.0 Å) with six nearest cations. The C–H···Br$^-$ bond lengths vary between 2.80(1) and 2.99(1) Å. One type of crystallographically independent cations forms long chains *via* weak edge to face π–π interactions. Furthermore, face to face π–π interactions are observed between certain cations of different chains.

Compound **2** is isostructural with the corresponding tetrabromo- and tetrachlorocuprate(II), and the tetrachloromanganate(II), -cobaltate(II) and -nickelate(II) compounds [44, 45]. The geometry of the

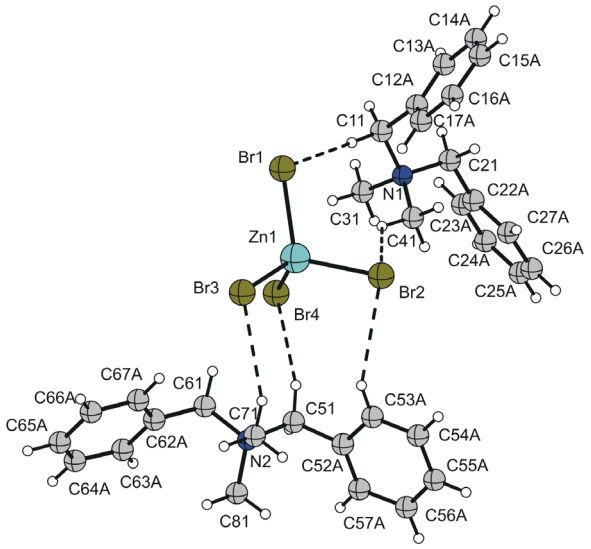

Fig. 5. Crystal structure of **5a** (isomorphous with compound **3**).

$CoBr_4^{2-}$dianion is close to tetrahedral (the average of the '*trans*' Br–Co–Br angle is 112.31(4)°) as it is the case with the $MnCl_4^{2-}$, $CoCl_4^{2-}$ and $NiCl_4^{2-}$ anions.

Compounds **3** and **5a** are isomorphous and crystallize from methanol in the monoclinic space group $P2_1/c$ with $Z = 4$. The asymmetric unit contains one MBr_4^{2-} anion and two $Bz_2Me_2N^+$ cations. The asymmetric unit of **5a** is presented in Fig. 5 as an example. One of the two crystallographically independent cations appears in the W-conformation, whereas the other one has a twisted conformation. The $CoBr_4^{2-}$ and $ZnBr_4^{2-}$ anions are almost perfectly tetrahedral with bond angles 107.23(5)–111.08(5)° and 107.09(3)–111.11(3)°, respectively.

The packing of the components is presented in Fig. 6b. One anion forms seven C–H···Br^- hydrogen bonds (C–H···Br^- < 3.0 Å) with four nearest cations (Fig. 6a). Furthermore, the packing is affected by weak intermolecular edge to face π–π interactions of the phenyl groups.

Compound **5b** crystallizes in the monoclinic space group $P2_1/c$ having one dianion and two cations in the asymmetric unit. The two crystallographically independent cations appear in twisted conformations. The anion is tetrahedrally coordinated, but the bond angles (102.76(3)–113.80(4)°) deviate more strongly from the ideal tetrahedral value than the bond angles of the $[MBr_4]^{2-}$ anions in compounds **1**–**5a** (Fig. 7).

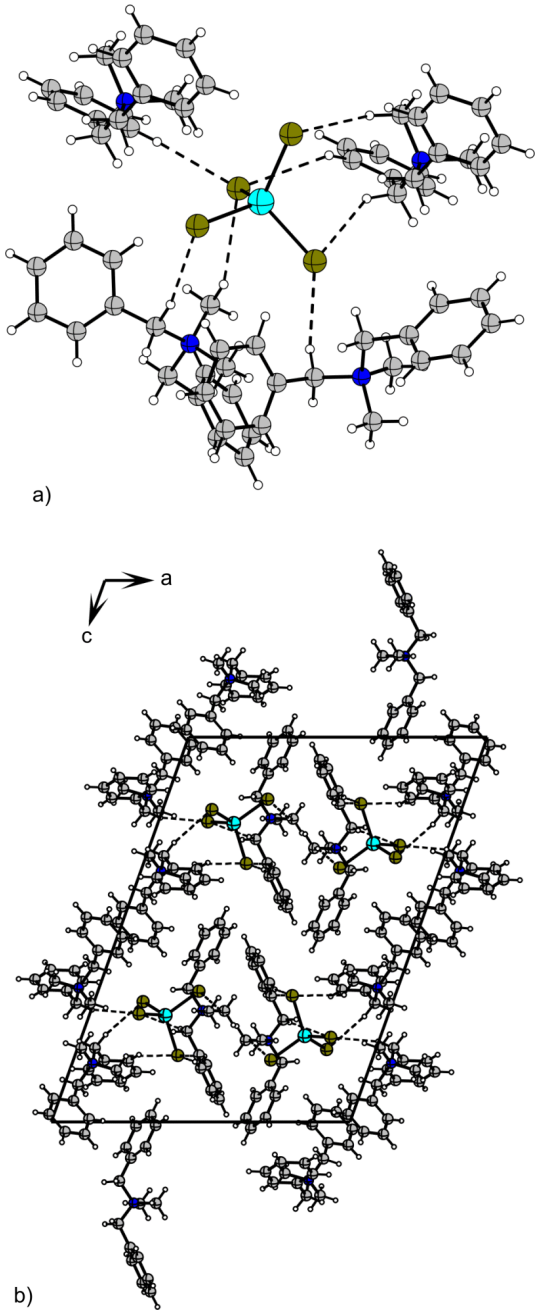

Fig. 6. a) The hydrogen bonding around the anions in **3** and **5a**. b) The packing of the components of compound **5a** (isostructural with **3**) viewed along the crystallographic *b* axis. The hydrogen bonds (C–H···Br^- < 3.0 Å) are shown as dashed lines.

The packing is stabilized by C–H···Br^- hydrogen bonds (C–H···Br^- < 3.0 Å). The anion forms eight C–H···Br^- bonds to five nearest cations; bond lengths

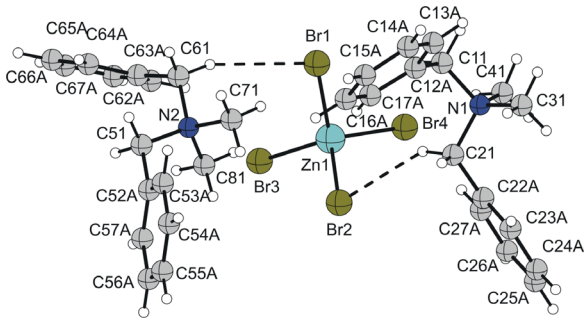

Fig. 7. The numbering scheme of compound **5b**. The dashed lines indicate the hydrogen bonds between the cations and the anion (C–H$\cdots$Br$^-$ $<$ 3.0 Å).

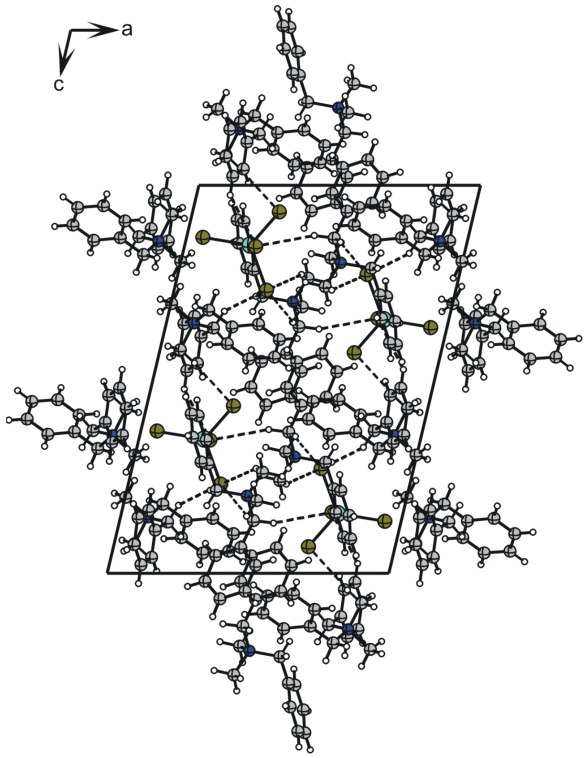

Fig. 8. The packing of the components of compound **5b**.

vary between 2.75(3) and 2.98(5) Å. Intermolecular edge to face and face to face π–π interactions can also be observed (Fig. 8).

Crystals **5a** and **5b** are two polymorphic forms containing no solvents. The former crystallizes from acetonitrile and the latter from methanol solution. The space group is the same for both **5a** and **5b**, but the packing is clearly different as shown in Fig. 9, viewed along the *b* axis. One type of the crystallographically independent cations of **5a** appears in the

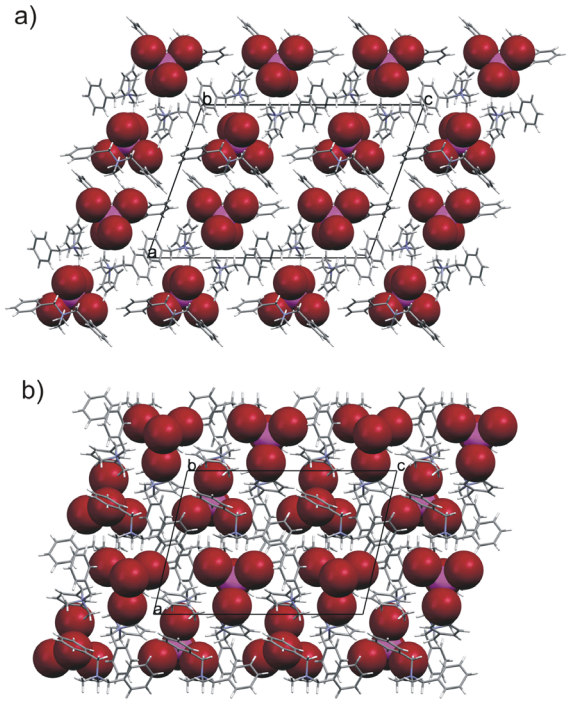

Fig. 9. The packing diagrams of the polymorphs **5a** and **5b**, viewed along the symmetry axes.

W-conformation, while the other type in **5a** and in both crystallographically independent cations of **5b** have a twisted conformation. In addition, the anion of **5a** is nearly tetrahedrally coordinated, whereas the coordination in the anion of **5b** deviates more strongly from the tetrahedral standard. The anion of **5a** interacts *via* seven C–H$\cdots$Br$^-$ bonds with four cations, whereas the anion of **5b** and the five surrounding cations interact *via* eight C–H$\cdots$Br$^-$ hydrogen bonds.

Thermal properties

Thermal decomposition paths and phase transitions for compounds **1**–**5** were determined by TG and DSC methods. The TG curves are presented in Fig. 10. Melting points (including the enthalpy changes) determined with DSC and decomposition ranges from TG measurements are compiled to Table 3.

All compounds melt around 200 °C showing a sharp melting peak in the DSC curve. No events other than the evaporation of the solvent molecules and the melting are observed in the DSC curves of **1**–**5** between −50 °C and the observed decomposition temperature.

In case of compounds **1** and **4**, which include cocrystallized acetonitrile and water, the loss of ace-

Table 3. Melting points (DSC onsets), enthalpy changes and decomposition ranges (the initial point of the decomposition) for compounds **1**–**5**.

Compound	T_m and Enthalpy change (°C, (Jg^{-1}))	Decomposition range (°C)
1	185.6 (45.6)	200–560
2	196.0 (33.4)	205–590
3	203.7 (48.5)	205–550
4	205.4 (68.6)	225–600
5a	206.7 (57.4)	225–600
5b	206.4 (60.7)	210–490

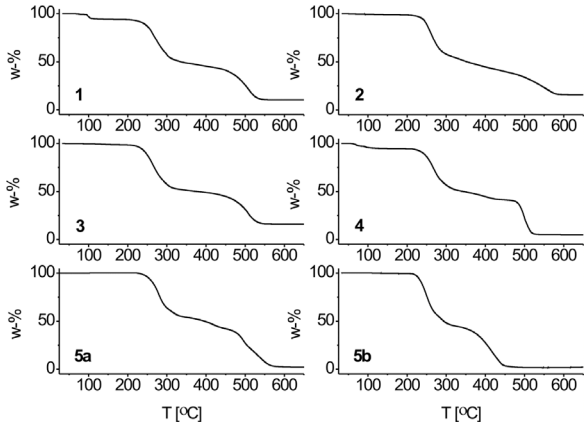

Fig. 10. The TG curves for compounds **1**–**5**.

tonitrile and water is observed over a rather wide temperature range of 60–90 °C (DSC curve). The related mass losses ($\Delta w - \%_{exp}$) of about 6% were observed in the TG curves, which correspond adequately to the calculated mass loss for both solvents (Δw_{calc} = 6.6–6.7%).

In case of compound **2** the loss of acetonitrile is not obvious in the TG curve as the evaporation of solvent occurs over a wider temperature range with an overall mass loss of only about 2% (Δw_{calc} = 2.4%). Correspondingly, a very modest rise of the baseline can be observed in the DSC curve.

Compounds **1**–**5** decompose mainly in two steps. The decomposition starts typically at 200–225 °C. In a first cleavage, the complexes decompose to metal(II) bromide and elemental carbon the latter of which is a result of a carbonization of the cation part. In the second stage a mixture of metal(II) bromide and metal(II) oxide are formed as final residues due to the air atmosphere, which was present in all TG experiments.

Conclusions

Bis[dibenzyldimethylammonium]tetrabromometallates or their solvates (with metals Mn, Co and Zn) crystallize with or without solvent molecules from acetonitrile, methanol and/or aqueous solutions. Not all compounds are isostructural unlike the previously reported corresponding tetrachlorometallates [45].

In $[(Bz_2Me_2N)_2][MnBr_4]\cdot CH_3CN\cdot H_2O$ (**1**) and $[(Bz_2Me_2N)_2][ZnBr_4]\cdot CH_3CN\cdot H_2O$ (**4**), acetonitrile and water molecules participate in a hydrogen bonding network. Both cations in the asymmetric unit are in the W-conformation like in Bz_2Me_2NBr [46]. The previously reported analogous tetrachlorometallate solvates [45] are isostructural with compound **2**. The solvent molecules fill the voids of the crystal structures and do not affect the packing. Isomorphous $(Bz_2Me_2N)_2CoBr_4$ (**3**) and $(Bz_2Me_2N)_2ZnBr_4$ (**5a**) crystallize in the monoclinic space group $P2_1/c$. The asymmetric unit consists of one crystallocraphically independent cation in a W-conformation, one independent cation in a twisted conformation and one dianion. Thus, the conformation of the other cation twists when the crystals of **3** and **5a** are formed. The second polymorph (**5b**) of compound **5** was obtained from aqueous solution and crystallizes in the same space group. However, the packing in the two polymorphs is different, as both cations in the asymmetric unit of **5b** appear in the twisted conformation.

In all crystals, the packing is stabilized by C–H···Br^- hydrogen bonds and weak intermolecular π–π interactions. In compounds **1** and **4,** the solvent molecules participate in the hydrogen bonding network by O–H···N, O–H···Br^- and C–H···Br^- interactions.

The coordination geometry of the $MX_4{}^{2-}$ ions is tetrahedral in all cases (**1**–**5**) as the Br–H–Br angles are close to 109.5 °C. A tetrahedral coordination sphere was also observed for previously reported $MCl_4{}^{2-}$ anions (M = Mn, Co, Ni or Zn) [45]. Thus, changing the halide from chloride to bromide does not affect the configuration of the $MX_4{}^{2-}$ anions. A flattening of the $MX_4{}^{2-}$ anions toward D_{2h} symmetry was observed for compounds with M = Cu and X = Br or Cl [44].

The average of the M(II)–Br distance is 2.503 Å for Mn, 2.412 Å for Co and 2.413–2.416 Å for Zn, as a consequence of the larger ionic radius of Mn compared Co, Ni and Zn [47].

The melting points of the title complexes (185.6 °C–206.7 °C) are very similar to those of the tetrachlorometallate solvate compounds (177.4 °C–201.6 °C) reported earlier [45]. All compounds start

to decompose shortly above the melting point and decompose mainly in two steps. In the first step the metal(II) halide and elemental carbon are formed, followed by the burning of elemental carbon, and part of the metal(II) halide ($[M\mathrm{Br}_4]^{2-}$ complexes) or all the metal(II)halide ($[M\mathrm{Cl}_4]^{2-}$ complexes) is converted into the corresponding metal(II)oxide.

Experimental Section

Syntheses

General procedure

Compounds **1**–**5** were crystallized from acetonitrile (**1**, **2** and **4**), methanol (**3**, **5a**) or water (**5b**) solutions containing stoichiometric amounts (2 : 1) of the $(\mathrm{Bz}_2\mathrm{Me}_2\mathrm{N})\mathrm{Br}$ salt and $M\mathrm{Br}_2$. Crystals were obtained by slow evaporation after a few days. $(\mathrm{Bz}_2\mathrm{Me}_2\mathrm{N})\mathrm{Br}$ was prepared as described earlier [46]. MBr_2 salts were used as received from manufacturers.

*$[Bz_2Me_2N]_2[MnBr_4]\cdot CH_3CN\cdot H_2O$ (**1**)*

Reagents: $(\mathrm{Bz}_2\mathrm{Me}_2\mathrm{N})\mathrm{Br}$ and $\mathrm{MnBr}_2\cdot 4\mathrm{H}_2\mathrm{O}$ in acetonitrile. Light yellow single crystals. Calcd. C 46.08, H 5.12, N 4.74; found C 45.70, H 4.76, N 4.47.

*$[Bz_2Me_2N]_2[CoBr_4]\cdot 0.5CH_3CN$ (**2**)*

Reagents: $(\mathrm{Bz}_2\mathrm{Me}_2\mathrm{N})\mathrm{Br}$ and anhydrous CoBr_2 in acetonitrile. Light blue single crystals. Calcd. C 46.53, H 4.91, N 4.11; found C 45.49, H 5.00, N 4.17.

*$[Bz_2Me_2N]_2[CoBr_4]$ (**3**)*

Reagents: $(\mathrm{Bz}_2\mathrm{Me}_2\mathrm{N})\mathrm{Br}$ and anhydrous CoBr_2 in acetonitrile solution. Blue single crystals. Calcd. C 46.24, H 4.85, N 3.37; found C 46.08, H 4.84, N 3.17.

*$[Bz_2Me_2N]_2ZnBr_4\cdot CH_3CN\cdot H_2O$ (**4**)*

Reagents: $(\mathrm{Bz}_2\mathrm{Me}_2\mathrm{N})\mathrm{Br}$ and anhydrous ZnBr_2 in acetonitrile. White single crystals. Calcd. C 45.54, H 5.06, N 4.69; found C 45.17, H 4.96, N 4.35.

*$[Bz_2Me_2N]_2[ZnBr_4]$ (**5a**)*

Reagents: $(\mathrm{Bz}_2\mathrm{Me}_2\mathrm{N})\mathrm{Br}$ and anhydrous ZnBr_2 in methanol. White single crystals. Calcd. C 45.88, H 4.81, N 3.34; found C 45.16, H 4.65, N 3.09.

*$[Bz_2Me_2N]_2[ZnBr_4]$ (**5b**)*

Reagents: $(\mathrm{Bz}_2\mathrm{Me}_2\mathrm{N})\mathrm{Br}$ and anhydrous ZnBr_2 in water. White single crystals. Calcd. C 45.88, H 4.81, N 3.34, found C 45.46, H 4.68, N 3.10.

Structure analyses

The X-ray single crystal structures for compounds **1**–**5** were determined with a Kappa APEX II diffractometer at −100 °C using graphite monochromaticed MoK_α (λ = 0.71069 Å) radiation. The data were processed with DenzoSMN v0.95.373 and the absorption correction was performed using Denzo [48]. All the structures were solved with Direct Methods (SIR97 [49]) and refined on F^2 by full-matrix least-squares techniques (SHELXL-97 [50]) using anisotropic displacement parameters. All hydrogen atoms (except the water hydrogens) were calculated to ideal positions as riding atoms by using isotropic displacement parameters. The water hydrogens were searched from the Fourier difference map and refined isotropically and later as riding atoms. Figs. 1–8 were drawn with the Diamond program [51] and Fig. 9 with the Mercury program [52].

CCDC 616208 – 616213 contains the supplementary crystallographic data for this paper. These data can be obtained free of charge from The Cambridge Crystallographic Data Centre via www.ccdc.cam.ac.uk/data_request/cif.

Thermal properties

Melting points of compounds **1**–**5** were determined on a Perkin Elmer PYRIS 1 DSC instrument. DSC measurements were carried out using 50 μL sealed aluminum sample pans with pinholes. The temperature calibration was carried out using three standard materials (*n*-decane, In, Zn) and the energy calibration by indium standard. The samples were heated under nitrogen atmosphere (flow rate of 50 mL min^{-1}) with the rate of 10 °C min^{-1} from −50 °C up to the predetermined (DSC, TG/DTA) decomposition temperature and then cooled to −50 °C with the rate of 10 °C min^{-1}. The heating-cooling cycle was repeated twice. The sample weights used in the measurements were about 3–6 mg.

The thermal decomposition pathways were followed with a Perkin Elmer TGA7 thermogravimetric analyzer. The measurements were carried out in platinum pans in air (flow rate 50 mL min^{-1}) with a heating rate of 10 °C min^{-1} in the temperature range 25–800 °C. The temperature calibration of the TGA equipment was carried out using the Curie-point technique (Alumel, Ni, Perkalloy, Fe). The weight balance was calibrated by measuring the standard weight of 50 mg at r. t. The sample weights used in the measurements were 1–8 mg.

Acknowledgements

We thank Ms. Elina Hautakangas for measuring the elemental analysis data. K. R. and S. B. gratefully acknowledge the financial support by the National Technology Agency (TEKES, proj. no. 40004/01), the Academy of Finland, the Foundation of Oskar Öflund, the Foundation of Magnus Ehrnrooth and the Foundation of Ellen and Artturi Nyyssönen.

[1] K. Hasebe, H. Mashiyama, S. Tanisaki, K. Gesi, *J. Phys. Soc. Jpn.* **1984**, *53*, 1866.
[2] M. R. Pressprich, M. R. Bond, R. D. Willett, *Phys. Rev.* **1991**, *B43*, 13549.
[3] M. R. Pressprich, M. R. Bond, R. D. Willett, *J. Phys. Chem. Solids* **2001**, *63*, 79.
[4] R. D. Willett, M. Wei, *J. Phys. Chem. Solids* **2000**, *61*, 2025.
[5] F. J. Zuniga, M. J. Cabezudo, G. Madariaga, M. R. Pressprich, M. R. Bond, R. D. Willett, *Acta Crystallogr.* **1991**, *B47*, 337.
[6] R. Perret, G. Godefroy, H. Arend, *Ferroelectrics* **1987**, *73*, 87.
[7] K. Gesi, *J. Phys. Soc. Jpn.* **1982**, *51*, 203.
[8] J. Sugiyama, M. Wada, A. Sawada, Y. Ishibashi, *J. Phys. Soc. Jpn.* **1980**, *49*, 1405.
[9] R. Nicholson, Y. Fujii, X. Chen, R. Willett, *J. Phys. Chem. Solids* **2001**, *62*, 933.
[10] K. Gesi, Izv. Akad. Nauk, *Ser. Fiz.* **2001**, *65*, 783.
[11] K. Gesi, *Kristallografiya* **1999**, *44*, 89.
[12] K. Gesi, *J. Phys. Soc. Jpn.* **2002**, *71*, 1376.
[13] K. Hasebe, H. Mashiyama, S. Tanisaki, *J. Phys. Soc. Jpn.* **1984**, *53*, 2326.
[14] C. L. Folcia, J. M. Perez-Mato, *Phys. Rev.* **1990**, *B42*, 8499.
[15] S. Tanisaki, H. Mashiyama, *J. Phys. Soc. Jpn.* **1980**, *48*, 339.
[16] R. D. Willett, J. A. Haugen, J. Lebsack, J. Morrey, *Inorg. Chem.* **1974**, *13*, 2510.
[17] D. R. Bloomquist, M. R. Pressprich, R. D. Willett, *J. Am. Chem. Soc.* **1988**, *110*, 7391.
[18] R. L. Harlow, W. J. Wells III, G. W. Watt, S. H. Simonsen, *Inorg. Chem.* **1974**, *13*, 2106.
[19] Z. Xiao, H. Chen, M. Shi, G. Wu, R. Zhou, Z. Yang, M. Wang, B. Tang, *Mat. Sci. Eng. B* **2005**, *117*, 313.
[20] T. J. Coffey, C. P. Landee, W. T. Robinson, M. M. Turnbull, M. Winn, F. M. Woodward, *Inorg. Chim. Acta* **2000**, *303*, 54.
[21] A. S. Albrecht, C. P. Landee, Z. Slanic, M. M. Turnbull, *Mol. Cryst. Liq. Cryst. Sci. Tech. Sect. A Mol. Crys. Liq. Cryst.* **1997**, *305*, 333.
[22] P. R. Hammer, D. C. Dender, D. H. Reich, A. S. Albrecht, C. P. Landee, *J. Appl. Phys.* **1997**, *81*, 4615.
[23] P. Zhou, J. E. Drumheller, G. V. Rubenacker, K. Halvorson, R. D. Willett, *J. Appl. Phys.* **1991**, *69*, 5804.
[24] T. Matsumoto, Y. Miyazaki, A. S. Albrecht, C. P. Landee, M. M. Turnbull, M. Sorai, *J. Phys. Chem. B* **2000**, *104*, 9993.
[25] C. P. Landee, M. M. Turnbull, C. Galeriu, J. Giantsidis, F. M. Woodward, *Phys. Rev.* **2001**, *B63*, 100402/1.
[26] R. D. Willett, C. Galeriu, C. P. Landee, M. M. Turnbull, B. Twamley, *Inorg. Chem.* **2004**, *43*, 3804.
[27] B. J. Hathaway, D. E. Billing, *Coord. Chem. Rev.* **1970**, *5*, 143.
[28] S. M. Ben-saber, A. A. Maihub, S. S. Hudere, M. M. Elajaily, *Microchem. J.* **2005**, *81*, 191.
[29] B. Barszcz, *Coord. Chem. Rev.* **2005**, *249*, 2259.
[30] B. Sui, J. Fan, T. Okamura, W. Sun, N. Ueyama, *Solid State Sci.* **2005**, *7*, 969.
[31] C. B. Aakeroy, J. Desper, J. Valdes-Martinez, *Cryst. Eng. Comm.* **2004**, *6*, 413.
[32] R. Keuleers, H. O. Desseyn, G. S. Papaefstathiou, L. Drakopoulou, S. P. Perlepes, C. P. Raptopoulou, A. Terzis, *Trans. Met. Chem.* **2003**, *28*, 548.
[33] N. S. Gill, R. S. Nyholm, P. Pauling, *Nature* **1958**, *182*, 168.
[34] G. Marcotrigiano, L. Menabue, G. C. Pellacani, *Trans. Met. Chem.* **1978**, *3*, 108.
[35] H. Suzuki, S. Ishiguro, H. Ohtaki, *J. Chem. Soc., Faraday Trans.* **1990**, *86*, 2179.
[36] S. Chaudhuri, T. Banerjee, P. N. Roy, G. Bocelli, M. K. D. Purkayastha, *Acta Crystallogr.* **1990**, *C46*, 385.
[37] H. Ishihara, S. Q. Dou, K. Horiuchi, H. Paulus, H. Fuess, A. Weiss, *Z. Naturforsch.* **1997**, *52a*, 550.
[38] G. Marcotrigiano, L. Menabue, G. C. Pellacani, *Trans. Met. Chem.* **1978**, *3*, 108.
[39] T. Wiest, H. Eickmeier, H. Reuter, R. Blachnik, *Z. Kristallogr. -NSC* **1999**, *214*, 394.
[40] G. S. Long, M. Wei, R. D. Willett, *Inorg. Chem.* **1997**, *36*, 3102.
[41] S. Haddad, R. D. Willett, *Inorg. Chem.* **2001**, *40*, 2457.
[42] H. Place, R. D. Willett, *Acta Crystallogr.* **1988**, *C44*, 34; and references therein.
[43] H. Place, R. D. Willett, *Acta Crystallogr.* **1987**, *C43*, 1050.
[44] S. Busi, M. Lahtinen, J. Valkonen, K. Rissanen, *J. Mol. Struct.* **2006**, *794*, 277.
[45] S. Busi, R. Fröhlich, M. Lahtinen, J. Valkonen, K. Rissanen, *Z. Naturforsch.* **2007**, *62b*, 28.
[46] S. Busi, M. Lahtinen, J. Ropponen, J. Valkonen, K. Rissanen, *Solid State Chem.* **2004**, *177*, 3757.
[47] R. D. Shannon, *Acta Crystallogr.* **1976**, *A32*, 751.
[48] (a) Z. Otwinowski, W. Minor, *Meth. Enzymol.* **1997**, *276*, 307; (b) Z. Otwinowski, D. Borek, W. Majewski, W. Minor, *Acta Crystallogr.* **2003**, *A59*, 228.
[49] A. Altomare, M. Burla, M. Camalli, G. Cascarano, C. Giacovazzo, A. Guagliardi, A. Moliterni, G. Polidori, R. Spagna, SIR97: A program for crystal structure solution, *J. Appl. Crystallogr.* **1999**, *32*, 115.
[50] G. M. Sheldrick, SHELXL–97 – A Program for Crystal Structure Refinement, University of Göttingen, Göttingen (Germany), **1997**.
[51] K. Brandenburg, DIAMOND, v 3.0b, Crystal Impact GbR Bonn, Germany, **2005**.
[52] I. J. Bruno, J. C. Cole, P. R. Edgington, M. K. Kessler, C. F. Macrae, P. McCabe, J. Pearson, R. Taylor, *Acta Crystallogr.* **2002**, *B58*, 389.